TDP2 protects transcription from abortive topoisomerase activity and is required for normal neural function

Fernando Gomez Herreros, Janneke H M Schuurs-Hoeijmakers, Mark McCormack, Marie T Greally, Stuart Rulten, Rocio Romero-Granados, Timothy J Counihan, Elijah Chaila, Judith Conroy, Sean Ennis, Norman Delanty, Felipe Cortes-Ledesma, Arjan P M de Brouwer, Gianpiero L Cavalleri, Sherif F El-Khamisy, Bert B A de Vries, Keith Caldecott

Publication date
01-05-2014

Document Version
Accepted version

Published in
Nature Genetics

Link to external publisher version
https://doi.org/10.1038/ng.2929

A Human 5'-Tyrosyl DNA Phosphodiesterase That Repairs Topoisomerase-Mediated DNA Damage

Felipe Cortes Ledesma[1,3*], Sherif F. El Khamisy[1,2,3], Maria C. Zuma[1], Kay Osborn[1], and Keith W. Caldecott[1*]

[1]Genome Damage and Stability Centre, University of Sussex, Science Park Road, Falmer, Brighton, Sussex, UK.
[2] Biochemistry Department, Faculty of Pharmacy. Ain Shams University, Cairo, Egypt

[3] these authors contributed equally
* to whom correspondence should be addressed

Topoisomerases regulate DNA topology and are fundamental to many aspects of chromosome metabolism[1, 2]. However, topoisomerase activity involves the transient cleavage of DNA, which if occurring close to sites of endogenous DNA damage or in the presence of topoisomerase poisons can result in abortive topoisomerase-induced DNA strand breaks[3-5]. A characteristic feature of topoisomerase-induced DNA breaks is covalent linkage of the enzyme to DNA termini via a 3'- or 5'-phosphotyrosyl bond. Such breaks are implicated in hereditary human disease[6-8], chromosomal instability and cancer[4, 9], and underlie the clinical efficacy of an important class of anti-tumour poisons[3, 9, 10]. The importance of liberating DNA termini from trapped topoisomerase is illustrated by the progressive neurodegenerative disease observed in individuals harbouring a mutation in *tyrosyl DNA phosphodiesterase-1* (TDP1), an enzyme that cleaves 3'-phosphotyrosyl bonds[6-8]. Surprisingly, however, a complementary human enzyme that cleaves 5'-phosphotyrosyl bonds has not been reported, despite the impact of DNA double-strand breaks harbouring such termini on chromosome instability and cancer[6-8]. Here, we identify such an enzyme in human cells and show that this activity efficiently restores 5'-phosphate termini at DNA double-strand breaks in preparation for DNA ligation. We reveal that this enzyme is TTRAP, a member of the Mg^{2+}/Mn^{2+}-dependent family of phosphodiesterases, and show that cellular depletion of TTRAP results in increased susceptibility and sensitivity to topoisomerase II-induced DNA double-strand breaks. TTRAP is the first human 5'-tyrosine phosphodiesterase to be identified and we suggest this enzyme additionally be denoted tyrosyl DNA phosphodiesterase-2 (TDP2).

In an attempt to identify novel human tyrosyl DNA phosphodiesterase activities, we exploited the hypersensitivity of *Saccharomyces cerevisiae tdp1Δ rad1Δ* double mutant cells to camptothecin (CPT), a topoisomerase I (Top1) poison that induces single-strand breaks (SSBs) with Top1 covalently linked to the 3'-terminus[3, 10]. This strain lacks not only Tdp1 but also Rad1-Rad10 nuclease, which in yeast provides an alternative (endonucleolytic) pathway for removing Top1 from 3'-termini[11, 12]. We transformed this strain with a human cDNA library

and screened the resulting population of transformants for cellular resistance to CPT. Of six *tdp1Δ rad1Δ* transformants displaying wild-type levels of CPT resistance, three harboured cDNA clones encoding TDP1 and three harboured cDNA clones encoding TTRAP (TRAF and TNF receptor-associated protein), a protein of unknown function and a putative member of the Mg^{2+}/Mn^{2+}-dependent phosphodiesterase super-family, with the DNA repair protein AP endonuclease-1 (APE1) being its closest relative[13, 14] (Fig.1a and Supplementary Fig.1).

The TDP1 and TTRAP cDNA clones recovered in the genetic screen suppressed the CPT sensitivity of *tdp1Δ rad1Δ* cells to a similar extent (Fig. 1b & data not shown). Whilst the pACT-TTRAP clones encoded TTRAP protein that lacked eight (pACT-TTRAP-2, pACT-TTRAP-3) or twenty-two (pACT-TTRAP-1) residues from the amino-terminus (data not shown), full-length TTRAP similarly suppressed the CPT sensitivity of *tdp1Δ rad1Δ* (Fig. 1c, left). In contrast, human APE1 protein failed to suppress this sensitivity, suggesting that ability to complement CPT sensitivity in *tdp1Δ rad1Δ* cells is not a generic feature of metal-dependent phosphodiesterases (Fig. 1c, left). Conversely, whereas human APE1 suppressed the sensitivity of AP endonuclease-defective *apn1Δapn2Δ tpp1Δ* yeast cells to methyl methanesulphonate (MMS)-induced DNA base damage, human TTRAP did not, suggesting that the impact of TTRAP in these experiments was restricted to topoisomerase-mediated DNA damage (Fig. 1c, right). TTRAP contains four highly conserved motifs that putatively assign this protein to the metal-dependent phosphodiesterase superfamily (see Fig.1a and Supplementary Fig.1). We thus examined whether mutation of two predicted catalytic residues (Fig.1a; E152 and D262) within two of these motifs impacted on the complementation of CPT sensitivity by TTRAP. Indeed, in contrast to wild-type TTRAP protein, neither $TTRAP^{E152A}$ nor $TTRAP^{D262A}$ restored CPT resistance in *tdp1Δ rad1Δ* cells (Fig. 1d).

We next purified recombinant human TTRAP, TDP1, and APE1 from *Escherichia coli* (Fig.2a, lanes 1-3) and incubated the purified proteins with a radiolabeled oligonucleotide duplex harbouring a nick with a single tyrosine covalently linked to the 3'-terminus via a phosphotyrosyl bond (Fig. 2a, inset). This is an established substrate for TDP1 that mimics the Top1-linked SSBs induced by CPT[6, 8]. As expected, TDP1 cleaved the 3'-phosphotyrosyl bond and thereby converted the 3'-tyrosine terminus to a 3'-phosphate (Fig.2a, lane 5). In contrast, recombinant human APE1 failed to do so (Fig.2a, lane 7). Notably, TTRAP cleaved the 3'-phosphotyrosyl bond, liberating DNA with a 3'-phosphate in a manner similar to TDP1, albeit

at much higher enzyme concentrations and less efficiently (Fig.2a, lane 6). TTRAP was also active on a DSB substrate harbouring a 3'-tyrosine (Fig.2b), albeit ~50-fold less efficiently and much slower than TDP1 (Fig.2d, left panel & Supplementary Fig.2). However, this activity was greatly reduced or absent in the absence of Mg^{2+}, consistent with a dependency on metal cofactor for TTRAP activity (Supplementary Fig.2). Moreover, the TTRAP activity detected here did not reflect a contaminant, because recombinant preparations of $TTRAP^{E152A}$ and $TTRAP^{D262A}$, purified in parallel with wild-type TTRAP, were largely or entirely inactive (Fig. 2b, lanes 6&7).We thus conclude that TTRAP possesses bona fide 3'-tyrosyl DNA phosphodiesterase activity, but that this activity is much weaker than that of TDP1, under the current experimental conditions at least.

In contrast to Top1, topoisomerase II (Top2) induces DNA double-strand breaks (DSBs) in which the topoisomerase is covalently linked via a phosphotyrosyl bond to the 5'-terminus of the break[9]. Surprisingly, a human enzyme that can preferentially or efficiently cleave DNA 5'-phosphotyrosyl bonds has not been reported, despite the established impact of this type of break on genetic stability and cancer[4, 9]. Given that the 3'-tyrosyl DNA phosphodiesterase activity of TTRAP was relatively weak, we wondered whether this enzyme might be a 5'-tyrosyl DNA phosphodiesterase. To address this possibility we employed a radiolabeled oligonucleotide duplex containing a DSB with a single tyrosine covalently linked to the 5'-terminus via a phosphotyrosyl bond (Fig.2c, inset). Strikingly, whereas neither human APE1 nor TDP1 cleaved the 5'-phosphotyrosyl bond, TTRAP led to complete conversion of the DSB terminus to a 5'-phosphate (Fig. 2c, lanes 2-4). That the 5'-terminus of the TTRAP reaction product was phosphate was confirmed using calf intestinal phosphatase, which converted the 5'-terminus of the reaction product to hydroxyl (Supplementary Fig.3a). Notably, TTRAP activity on the 5'-phosphotyrosyl substrate was largely or entirely absent in reactions that lacked Mg^{2+} and contained EDTA (Supplementary Fig.3b), or in reactions containing the phosphodiesterase mutant proteins $TTRAP^{E152A}$ or $TTRAP^{D262A}$ (Fig.2c, lanes 5&6). Importantly, similar to TDP1 activity on 3'-phosphotyrosyl termini, the activity of TTRAP on 5'-phosphotyrosyl termini was robust and rapid (Fig.2d and Supplementary Fig.3c&3d). In contrast, TTRAP was not active on a substrate containing an internal abasic site, a preferred substrate of APE1, or on 5'-AMP DNA termini, a preferred substrate of Aprataxin

(Supplementary Fig.4). We conclude from these experiments that TTRAP is a bona fide 5'-tyrosyl DNA phosphodiesterase.

We next examined whether we could detect 5'-tyrosyl DNA phosphodiesterase activity in human whole cell extracts. Indeed, such activity was readily detected in A549 cell extract (Fig. 3a, lanes 1-5). Moreover, this activity was reduced by ~50% in A549 cells in which TTRAP was depleted by ~80% by RNAi, and was increased by addition of recombinant human TTRAP (Fig.3). However, 5'-tyrosyl DNA phosphodiesterase activity in TTRAP-depleted extracts was not increased by addition of recombinant TTRAP^{D262A} or TTRAP^{E152A} (Supplementary Fig.5). Notably, wild-type and TTRAP-depleted A549 extracts displayed similar levels of metal-independent 3'-tyrosyl DNA phosphodiesterase activity and were equally able to repair a gapped DNA duplex that lacked damaged termini, suggesting that TTRAP-depleted extracts are competent for other types of DNA repair activity (Supplementary Fig.5). These data indicate that human whole cell extract possesses robust 5'-tyrosyl DNA phosphodiesterase activity, and suggest that TTRAP is a major source of this activity.

Finally, we examined whether the 5'-tyrosyl DNA phosphodiesterase activity of TTRAP fulfils a role in protecting against topoisomerase-induced DNA damage, *in vivo*. We first noted that over-expression of TTRAP, but not of TDP1, mutant TTRAP^{D262A}, or TTRAP^{E152A}, measurably increased the resistance of *ISE2* cells, a strain of *S.cerevisiae* with increased drug permeability[15], to the Top2 poison, etoposide (Fig.4a and Supplementary Fig.6). We also noted that GFP-tagged TTRAP accumulated in nuclear PML bodies, as reported previously[16], and more importantly at sites of laser-induced UVA damage (Fig.4b), consistent with a role for TTRAP in DNA repair. That this accumulation was relatively weak may reflect that topoisomerase-induced DNA breaks are likely only a minor component of UVA laser-induced DNA damage[17-19]. We next examined the impact of TTRAP depletion on the sensitivity of human A549 cells to different types of DNA damage. Whereas TTRAP depleted cells (see Fig.3 for a typical level of depletion) exhibited little or no sensitivity to CPT or MMS (Supplementary Fig.7), these cells were markedly hypersensitive to etoposide (Fig. 4c). These data provide compelling evidence that TTRAP is required during the repair of Top2-induced DSBs in human cells. To explore this possibility further, we examined whether TTRAP depletion resulted in the accumulation of DNA strand breaks during exposure to topoisomerase poisons. Notably, TTRAP depletion failed to increase the accumulation of DNA strand breaks

during incubation with CPT (a Top1 poison), as measured either by alkaline-comet assays (Supplementary Fig.7) or the appearance of γ-H2AX foci (Fig.4d). This contrasted with the >10-fold increase in DNA strand breaks observed in MEFs lacking Tdp1, which is the primary cellular 3'-tyrosyl DNA phosphodiesterase activity (Supplementary Fig.7). However, treatment with etoposide resulted in accumulation of ~2-fold more γH2AX foci in TTRAP-depleted cells than in mock-depleted control cells (Fig.4d). In addition, over-expression of wild-type TTRAP, but notably not $TTRAP^{D262A}$ or $TTRAP^{E152A}$, reduced levels of etoposide-induced γH2AX foci in transiently-transfected A549 cells (Fig.4e and Supplementary Fig.7). Together, these data support the notion that the 5'-tyrosyl DNA phosphodiesterase activity of TTRAP is required for efficient repair of Top2-induced chromosomal DSBs.

It is noteworthy that 5'-tyrosyl DNA phosphodiesterase activity of TTRAP can enable the repair of Top2-induced DSBs without the need for nuclease activity, creating a 'clean' DSB with 5'-phosphate termini that are ready for ligation. This contrasts with currently established mechanisms for DSB repair, which involve structure-specific nucleases such as CtIP and MRN to 'trim' DSB termini[20, 21]. TTRAP may thus provide an 'error-free' mechanism for direct end-joining of Top2-induced DSBs, a process that might have particular utility for maintaining genetic stability in long-lived non-cycling cells.

In summary, we reveal that human TTRAP is a bona fide 5'-tyrosyl DNA phosphodiesterase and we demonstrate that this enzyme is required for efficient repair of Top2-induced DNA double-strand breaks. Since TDP1 and TTRAP are complementary activities, together providing cells with an ability to remove trapped topoisomerase from both 3'- and 5'-DNA termini, we suggest that TTRAP be additionally designated Tyrosyl DNA Phosphodiesterase-2 (TDP2). It will now be of interest to determine how the tyrosyl DNA phosphodiesterase activity of TTRAP/TDP2 relates to the reported involvement of this protein in transcriptional regulation, apoptosis, and embryonic development[13, 22-24]. Given the central role fulfilled by topoisomerases in chromosome metabolism, our findings suggest that TTRAP/TDP2 may have additional important functions in many aspects of cell biology, including the suppression of chromosome instability and cancer.

Acknowledgements

This work was funded by the MRC (G0600776), BBSRC (BB/C516595/1), and CR-UK (C6563/A10192). SFEK and FCL were also funded by Fellowships from the Wellcome Trust (SFE; 085284), Marie Curie (FCL; 2007-2-1-IEF-221222), and EMBO (FCL; ALTF 956-2006).

Author Contributions

FCL developed the genetic screen and conducted the mammalian cell experiments. MCZ and FCL conducted the yeast experiments. KO and SFEK prepared the recombinant proteins and SFEK conducted the biochemical experiments. KWC, FCL, and SFEK designed and interpreted the experiments. KWC coordinated the project and wrote the manuscript.

Figure legends

Figure 1: Human TTRAP suppresses the sensitivity of yeast to topoisomerase I-induced DNA damage.

a, Cartoon of TTRAP. **b,** TTRAP suppresses CPT sensitivity in *tdp1Δrad1Δ* yeast. Serial dilutions of wild-type (left) and *tdp1Δrad1Δ* (right) cells harbouring pACT-TDP1-1, pACT-TTRAP-2 or pACT vector were plated onto media lacking (-) or containing (+) 20μM CPT. **c,** Human APE1 or TTRAP do not suppress the sensitivity of *tdp1Δrad1Δ* or *apn1Δapn2Δ tpp1Δ* cells to CPT or MMS. Serial dilutions of *tdp1Δrad1Δ* (left) and *apn1Δapn2Δ tpp1Δ* (right) transformed with pGBKT7-TTRAP, pAS-APE1 or pGBKT7 vector were plated onto media lacking (-) or containing (+) 20μM CPT or 100μM MMS. **d,** Mutant TTRAP fails to suppress CPT sensitivity. Wild-type (left) or *tdp1Δrad1Δ* (right) cells transformed with pVTU260 vector or pVTU260 encoding full-length wild-type or mutant (E152A or D262A) TTRAP were analysed for CPT sensitivity as above.

Figure 2: TTRAP Possesses 3'- and 5'-tyrosyl DNA phosphodiesterase (TDP) activity.

a, 3'-TDP activity of TTRAP at SSBs. *Lanes 1-3*, Analysis of recombinant proteins by SDS-PAGE. *Lanes 4-7*, ^{32}P-radiolabeled 43-mer duplex (50nM) harbouring a nick with a tyrosine (Y) linked to the 3'-terminus of the labelled 18-mer (inset, top) was incubated for 1-hr at 37°C in the absence ("-") or presence of the indicated human proteins and analysed by denaturing PAGE/phosphorimaging. Positions of ^{32}P-radiolabeled substrate (18-Y) and product (18-P) are indicated. An 18-mer with a 3'-OH terminus (18-OH) was included as a marker ("3'OH"). **b,** 3'-TDP activity of TTRAP at DSBs. *Lanes 1-3*; Analysis of human TTRAP ("WT"), TTRAP^{D262A} ("D"), or TTRAP^{E152A} ("E") by SDS-PAGE. *Lanes 4-8*; ^{32}P-radiolabeled 18-mer duplex (50nM) harbouring a DSB with a tyrosine (Y) linked covalently to the 3'-terminus of the labelled 18-mer (inset, *top*) was incubated as above in the absence ("-") or presence of the indicated proteins (1μM). **c,** 5'-TDP activity of TTRAP at DSBs. ^{32}P-radiolabeled 19-mer duplex (50nM) harbouring a DSB with a tyrosine (Y) linked covalently to the 5'-terminus of the labelled 19-mer (inset, *top*) was incubated with of the indicated human proteins (150nM) as above. Positions of ^{32}P-radiolabeled substrate (Y-19) and repair product (P-19) are indicated. A 19-mer with a 5'-OH terminus (OH-19) was included as a marker ("5'OH"). **d,** *left,* the 3'-TDP substrate (50nM) in panel b was incubated with human TDP1 (0, 4.5, 9, 36, 90nM) or TTRAP (0, 36, 90, 225, 450, 900nM) for 1-hr at 37°C. *Right*, the 5'-TDP substrate (50nM) in panel c was incubated with TTRAP (0, 15, 30, 60, 240nM) or 400nM TDP1 for 1hr at 37°C. Reaction products were quantified using ImageQuant and data are the mean (±1 s.e.m) of 3 experiments.

Figure 3: Reduced 5'-TDP activity in TTRAP-deficient human cell extracts.

Extract from A549 cells transfected with pSuper ("pS") or pSuper-TTRAP ("pS-TT") was incubated for the indicated time with a ^{32}P-radiolabeled 20-mer duplex harbouring a DSB with a tyrosine (Y) linked covalently to the 5'-terminus of the labelled 20-mer (inset, top). Reaction products were analysed by denaturing PAGE/phosphorimaging. The position of ^{32}P-radiolabeled substrate (Y-20), repair product (P-20), and 20-mer 5'-OH marker (OH-20) are indicated. The % substrate converted to reaction product was quantified (mean±1s.e.m, n=4) using ImageQuant (*bottom right*). *Top right*; Western blot

of XRCC1 ("X") and TTRAP ("TT") in the cell extracts employed above. Asterisk denotes non-specific band.

Figure 4: TTRAP effects etoposide sensitivity and DNA damage accumulation.

a, TTRAP increases etoposide resistance in yeast. Ten-fold serial dilutions of *ISE2 S. cerevisiae* transformed with pACT-TDP1-1, pACT-TTRAP-2 or pACT vector were plated onto medium containing 500μM etoposide. **b**, GFP-TTRAP accumulates at sites of UVA damage. Human A549 cells transiently-transfected with pEGFP-TTRAP were damaged with a UVA laser and eGFP imaged at the indicated times (min) (arrow denotes position of laser track). **c**, TTRAP-depletion results in etoposide hypersensitivity. A549 cells transfected with pSuper ("pS") or pSuper-TTRAP ("pS-TT") were treated with etoposide and surviving colonies counted. **d,** TTRAP-depletion increases accumulation of etoposide-induced DSBs. A549 cells transfected with pSuper or pSuper-TTRAP were treated with CPT (10 μM) or etoposide (10 μM) for 16 h and the average number of γH2AX foci/cell quantified. Data are the mean (± 1s.e.m) of three experiments. **e,** TTRAP over-expression decreases accumulation of etoposide-induced DSBs. A549 cells transiently-transfected with pcDNA3.1His-TTRAP, pcDNA3.1His-TTRAP^{D262A} ("D"), or pcDNA3.1His-TTRAP^{E152A} ("E") were treated with etoposide as above and the average number of γH2AX foci quantified in cells either over-expressing recombinant TTRAP (open bars) or lacking visible recombinant TTRAP (filled bars). Data are the mean (±1s.e.m) of three experiments**.** Asterisks denote statistically significant (paired t-test p<=0.05) differences.

Methods Summary

Human TTRAP was recovered in a genetic screen for restoration of CPT resistance in *tdp1Δ rad1Δ* budding yeast cells by transformation with 16 μg of a pACT human cDNA library and plated on appropriate medium supplemented with 20μM CPT (Sigma). For sensitivity assays, transformants were re-suspended in 200 μl sterile H_2O and 10 μl drops of 10-fold serial dilutions were plated onto medium lacking or containing the appropriate drug. The generation of oligonucleotide duplexes employed for in vitro assays, DNA constructs employed for expression of TTRAP in yeast, *E.coli*, and mammalian cells, and the pSuper

constructs employed for shRNA mediated depletion of TTRAP, are described in detail in the Methods section. The recombinant human APE1, TDP1, and TTRAP proteins employed for in vitro assays were expressed in *E.coli* and purified by immobilised metal-chelate chromatagoraphy (IMAC) followed by ion exchange chromatography. The products of in vitro reactions were fractionated by denaturing PAGE and detected by phosphorimaging. The detection of EGFP-TTRAP accumulation at sites of UVA laser damage was achieved by seeding transfected A549 cells onto glass-bottom coverslips followed by incubation with Hoechst 33258 dye and irradiation with a 351-nm UVA laser (approximately 0.35 J/m2) using a Zeiss Axiovert. For clonogenic survival assays, A549 cells were plated into 10-cm dishes in duplicate and incubated at 37°C for 4h. Cells were then mock-treated or treated in medium at 37°C with genotoxin (Sigma) for 1-3 hr and then incubated at 37°C in drug-free medium for 14 days to allow formation of macroscopic colonies. DNA strand breaks were quantified using the alkaline comet assay and by quantification of γH2AX foci.

Methods (Full)

Yeast strains, screening and sensitivity assays

All yeast strains used in this study have been previously described. Wild type (YW465), *tdp1Δ rad1Δ* (YW812) and *apn1Δ apn2Δ tpp1Δ* (YW778) were kindly provided by Dr. Thomas E. Wilson[11, 25]. *ISE2* (JN362a) strain is a gift of Dr. Mathew Neale, originally obtained from Dr. John Nitiss[26]. Screening of a human cDNA library was performed as follows. Yeast *tdp1Δ rad1Δ* cells were transformed with 16 µg of pACT human cDNA library[27] and plated on Synthetic Complete medium lacking leucine (SC-Leu) supplemented with 20µM CPT (Sigma). A total number of $7.5x10^5$ clones were screened, as estimated from the transformation efficiency on SC-Leu lacking CPT. Healthy-looking colonies were isolated after 7 days, rescreened for growth in 20µM CPT, and their pACT construct isolated from *E. coli*. The phenotype was confirmed after retransforming these constructs into *tdpΔ rad1Δ* cells. Three full-length TDP1 clones were identified (denoted pACT-TDP1-1, -2 and -3), comprising nucleotides 234-2069, 97-2090 and 1-2101, respectively, of the published transcript variant 1 cDNA (NM_018319). Three incomplete clones of TTRAP were identified, one comprising nucleotides 90-1884 (pACT-TTRAP-1), and two comprising nucleotides 49-1889 (pACT-

TTRAP-2 and -3) of the published cDNA sequence (NM_016614.2). For sensitivity assays, equal-sized colonies of the corresponding transformants were re-suspended in 200 µl sterile H_2O and 10 µl drops of 10-fold serial dilutions were plated onto SC-Leu (for pACT transformants), SC-tryp (for pAS/pGBKT7 transformants), or SC-Ura (for pVTU260 transformants) media lacking or containing the appropriate drug.

DNA constructs

Full-length TTRAP ORF, flanked by *NdeI* and *BamHI* restriction sites, was cloned into pCRII-TOPO (Invitrogen) after PCR amplification from pACT-TTRAP-2 using the following primers (Operon) (the region of TTRAP missing from pACT-TTRAP-2 and included in the primer is underlined): [5'-AGG AAG CAT ATG GAG TTG GGG AGT TGC CTG GAG GGC GGG AGG GAG GCG GCG G-3'] (forward) and [5'-TGC AAC GGA TCC AAT CAG GGC AAA ACC CAC AC-3'] (reverse). Mutations were introduced into pCRII-TTRAP using Quickchange XL site-directed mutagenesis kit (Stratagene) using primers [5'-CCA GAT GTG ATA TTT CTA CAG GCA GTT ATT CCC CCA TAT TAT AGC-3'] (forward)/[5'-GCT ATA ATA TGG GGG AAT AAC TGC CTG TAG AAA TAT CAC ATC TGG-3'] (reverse) for $TTRAP^{E152A}$ and [5'-GCT ACA GTT ATA TTT GCA GGA GCT ACA AAT CTA AGG GAT CGA GAG-3'] (forward)/ [5'-CTC TCG ATC CCT TAG ATT TGT AGC GCC TGC AAA TAT AAC TGT AGC-3'] (reverse) for $TTRAP^{D262A}$. pGBKT7 (Clontech) and pET16b (Novagen) constructs expressing TDP1 were previously described[6]. pGBKT7 (Clontech) and pET16b (Novagen) constructs expressing wild-type TTRAP, $TTRAP^{E152A}$, and $TTRAP^{E262A}$ were created by sub-cloning the TTRAP ORF from the appropriate pCRII-TOPO construct using *NdeI* and *EcoRI*. Untagged full-length human TTRAP yeast expression vectors were created by cloning the appropriate TTRAP ORF from pCRII-TOPO (*NdeI-BamHI*) into *NheI-BamHI* of pVTU260 (Euroscarf, kindly provided by Dr. Eva Hoffmann). pET16b-APE1 has been described previously[28], and APE1 ORF was cloned into *BamHI-EcoRI* sites of pAS2-1 (Clontech). pEGFP-TTRAP was created by cloning a *BamHI-EcoRI* fragment of pACT-TTRAP-2 into *BglII-EcoRI* of pEGFP-C3 (Clontech). Mammalian TTRAP expression constructs were created by cloning the appropriate TTRAP ORF from pCRII-TOPO into pcDNA3.1-HisC (Invitrogen) using *EcoRI*. For pSuper-TTRAP, the following oligonucleotides (Operon) containing an appropriate 19-bp region of homology to TTRAP (underlined) were

annealed and sub-cloned into *BglII-HindIII* sites of pSuper (OligoEngine): [5'-GAT CCC CGT ACA GCC CAG ATG TGA TAT TCA AGA GAT ATC ACA TCT GGG CTG TAC TTT TTA-3'] (forward) and [5'-AGC TTA AAA AGT ACA GCC CAG ATG TGA TAT CTC TTG AAT ATC ACA TCT GGG CTG TAC GGG-3'] (reverse).

Purification of recombinant human proteins and human cell extracts

Amino-terminal histidine-tagged recombinant human TTRAP, $TTRAP^{D262A}$, $TTRAP^{E152A}$, TDP1, and APE1 were expressed from pET16b in BL21 (DE3) cells and purified by immobilised metal-chelate chromatography (IMAC) and ion exchange chromatography. Proteins were then dialysed in buffer comprised of 25mM Tris-Cl pH 7.5, 1mM DTT, 10% glycerol, and either 100mM NaCl or 130mM KCl. Purified human proteins were quantified on Coomassie blue stained polyacrylamide gels by comparison to BSA standards and verified by Bio-Rad Protein Assay Kit. Human whole cell extracts were prepared from $3x10^6$ A549 cells by lysis in 0.1ml of 20mM Tris-HCl (pH7.5), 10mM EDTA, 1mM EGTA, 100mM NaCl, 1% triton-X100 and protease inhibitor cocktail (Sigma). The extract was clarified by centrifugation and quantified using a Bio-Rad Protein Assay Kit with BSA employed as a standard.

Preparation of DNA substrates and in vitro repair reactions

Gel-purified oligonucleotides were 5'-labelled with ^{32}P using [γ-^{32}P] ATP and T4 PNK or 3'-labelled using [α-^{32}P] dCTP and klenow DNA polymerase as described below. For the 19-mer DSB 5'-phosphotyrosyl substrate, a 5'-Y-18-mer [5'-Y-TCC GTT GAA GCC TGC TTT-3'] (Midland Certified Reagent Company, TX) was annealed with a 19-mer [5'-GAA AGC AGG CTT CAA CGG A-3'] and the resulting 1-bp 5' overhang filled-in with [α-^{32}P] dCTP and klenow DNA polymerase. For the 20-mer 5'-phosphotyrosyl DSB substrate (used in reactions employing whole cell extract) the 5'-Y-18-mer (above) was annealed to the 20-mer [5'-AGA AAG CAG GCT TCA ACG GA-3'] and the resulting 2-bp 5' overhang filled-in as described above but using [α-^{32}P] dCTP and ddTTP, to inhibit degradation of the radiolabeled oligonucleotide by non-specific nucleases. For the 43-mer 3'-phosphotyrosyl SSB (nick) substrate, a radiolabeled 3'-Y-18-mer [^{32}P-5'-TCC GTT GAA GCC TGC TTT-Y-3'] (Kindly provided by Howard Nash) was annealed with a 25-mer [5'-GAC ATA CTA ACT TGA GCG

AAA CGG T-3'] and a 43-mer [5'-CCG TTT CGC TCA AGT TAG TAT GTC AAA GCA GGC TTC AAC GGA T-3']. For the 18-mer 3'-phosphotyrosyl DSB substrate, the radiolabeled 3'-Y-18-mer (above) was annealed with the 19-mer [AAA GCA GGC TTC AAC GGA T]. For the AP endonuclease substrate, a 39-mer [5'-GCG CAG CTA GCG GCG GAT GGC XCC GTT GAA GCC TGC TTT-3'] containing an abasic site (X) obtained from Eurofins was 5'-labelled with ^{32}P and then annealed to a 40-mer [5'-GAA AGC AGG CTT CAA CGG AGC CAT CCG CCG CTA GCT GCG C-3']. 5'-AMP substrates were prepared as described previously[29]. Reactions were initiated by mixing 4µl of an appropriate dilution (in protein dialysis buffer) of the indicated recombinant human protein, or 4µl of whole cell extract (16µg total protein), with 4µl of 2X Master Mix (50mM HEPES pH8.0, 260mM KCl, 2mM DTT and, unless otherwise indicated, 20mM $MgCl_2$) containing 100nM (for recombinant protein experiments) or 300nM (for cell extract experiments) of the appropriate ^{32}P-labelled oligonucleotide duplex. For experiments employing cell extract, 150µM competitor single-stranded oligonucleotide [5'-CTAACTTGAGCGAAACGGT-3'] was present to reduce non-specific nucleolytic degradation of the duplex substrate. All reactions were terminated by addition of formamide loading buffer and fractionated by denaturing PAGE.

Cells, cell culture and transfection

A549 cells were cultured in Dulbecco's minimal essential medium (Gibco, Invitrogen) supplemented with 15% foetal calf serum and 1% glutamine. Cells were transfected using Genejuice (Novagene) according to the manufacturer's instructions. For the generation of wild-type and *Tdp1*$^{-/-}$ mouse embryonic fibroblasts, *Tdp1*$^{-/+}$ animals were mated and 14-day embryos were dissociated, trypsinised, and plated in DMEM with 10% FCS. Genotyping for the mutant *Tdp1* allele was performed on cell pellets, essentially as described [30]. For shRNA-mediated depletion of TTRAP, A549 lung carcinoma cells were co-transfected with 2µg of pCD2E vector encoding G418 resistance and 1µg of either pSuper or pSuper-TTRAP. After selection in 1.5mg/ml G418 (Gibco, Invitrogen) for 6 days, cells were harvested for analysis.

Immunoblotting, immunoflourescence and antibodies

For Western blots, cells (10,000/µl) were lysed in SDS-PAGE loading buffer and incubated at 90°C for 5 min. Whole-cell extracts were fractionated by SDS-PAGE and transferred to

nitrocellulose. Membranes were blocked for 1 h in PBS-Tween 20 (PBST) containing 5% non-fat dried milk (NFDM) and then incubated for 2h with anti-XRCC1 Mab (33-2-5) or affinity-purified anti-TTRAP polyclonal antibody (SY1340) at 1/100 or 1/200 dilution, respectively, in PBST + 5%NFDM. Membranes were rinsed in PBST and incubated in PBST + 5%NFDM containing horseradish peroxidase-conjugated anti-rabbit IgG or anti-mouse IgG (DAKO), as appropriate, at a 1/3,000 dilution for 1h at room temperature. Membranes were then rinsed with PBST and antibody complexes detected by enhanced chemiluminescence (Amersham). Note that the αTTRAP polyclonal antibody was raised in rabbit by Eurogentec against full-length recombinant human TTRAP expressed in *E. coli*. For immunofluorescence analysis, cells were grown on coverslips, rinsed in PBS, fixed with 4% paraformaldehyde for 5min at RT, permeabilized with 0.2% Triton X-100, and after rinsing in PBS (x2) blocked in PBS +5% BSA. Cells were then incubated with appropriate primary antibodies in PBS + 1%BSA for 1 h at RT. Anti-γH2AX (Ser139) Mab (Upstate) and anti-TTRAP rabbit polyclonal antibody (Abcam, ab33246) were used at 1/800 and 1/200 dilution respectively. After rinsing in PBST (x3), cells were incubated for 30 min RT in PBS + 1% BSA containing appropriate secondary antibody (Alexa Fluor 555 goat anti-mouse IgG and Alexa Fluor 488 goat anti-rabbit IgG, Invitrogen) at a 1/200 dilution and then rinsed again (x3) in PBST. Cells were counterstained with 4',6'-diamidino-2-phenylindole (DAPI) and mounted with Vectashield (Vecta Laboratories).

Laser microirradiation

A549 cells were seeded onto glass-bottom coverslips (MatTek), transfected with 1μg of pEGFP-TTRAP and 24h later pre-incubated for 10 min with 10 μg/ml Hoechst dye 33258 at 37°C. Selected cells were then irradiated with a 351-nm UVA laser (approximately 0.35 J/m2) focused through a 40x/1.2-W objective using a Zeiss Axiovert equipped with LSM 520 Meta, and images were taken every minute following irradiation.

Clonogenic survival assays

A549 cells transfected with empty pSuper or with pSuper-TTRAP as described above were plated into 10-cm dishes (1,000 per plate) in duplicate and incubated at 37°C for 4h. Cells were mock-treated or treated in medium at 37°C with the indicated concentration of CPT or

etoposide for 3h, or with MMS for 1h. All drugs were from Sigma. Cells were then rinsed in PBS and incubated at 37°C in drug-free medium for 14 days. Colonies were fixed with 90% ethanol and stained with 1% methylene blue. Survival was calculated as a percentage, using the equation Nt/Nu x 100, where Nt and Nu are the number of colonies on treated and untreated plates, respectively. Data are shown as the mean (±1SEM) of at least three independent experiments.

Alkaline single-cell agarose gel electrophoresis (comet) assays

DNA strand breaks were quantified using the alkaline comet assay as described previously[6]. Average tail moments from 100 cells per sample were obtained using Comet Assay III software (Perceptive Instruments), and data are shown as the mean (±1SEM) of at least three independent experiments.

γH2AX assays

Cells were mock-treated or treated with the indicated drug at the indicated concentration. Following γH2AX immunofluorescence staining, the average number of γH2AX foci/cell was determined from fifty cells/sample using a Nikon Eclipse 50i microscope at x100 magnification. Over-expression experiments were carried out as described above except that cells were transfected with 250ng of the appropriate pcDNA3.1-His construct 1 day prior incubation with the drug. 15-40 cells/sample were scored, depending on the number of cells highly over-expressing TTRAP (see Supplementary Figure 7 for representative examples). Data are the mean ± 1SEM of three independent experiments.

1. **Champoux, J. J. DNA topoisomerases: structure, function, and mechanism. Annu Rev Biochem 70, 369-413 (2001).**
2. **Wang, J. C. Cellular roles of DNA topoisomerases: a molecular perspective. Nat Rev Mol Cell Biol 3, 430-40 (2002).**
3. **Li, T. K. & Liu, L. F. Tumor cell death induced by topoisomerase-targeting drugs. Annu.Rev.Pharmacol.Toxicol. 41, 53-77 (2001).**

4. **Deweese, J. E. & Osheroff, N. The DNA cleavage reaction of topoisomerase II: wolf in sheep's clothing. Nucleic Acids Res 37, 738-48 (2009).**
5. **Pourquier, P. & Pommier, Y. Topoisomerase I-mediated DNA damage. Adv Cancer Res 80, 189-216 (2001).**
6. **El-Khamisy, S. F. et al. Defective DNA single-strand break repair in spinocerebellar ataxia with axonal neuropathy-1. Nature 434, 108-113 (2005).**
7. **Takashima, H. et al. Mutation of TDP1, encoding a topoisomerase I-dependent DNA damage repair enzyme, in spinocerebellar ataxia with axonal neuropathy. Nat.Genet. 32, 267-272 (2002).**
8. **Yang, S. W. et al. A eukaryotic enzyme that can disjoin dead-end covalent complexes between DNA and type I topoisomerases. Proc.Natl.Acad.Sci.U.S.A 93, 11534-11539 (1996).**
9. **Nitiss, J. L. Targeting DNA topoisomerase II in cancer chemotherapy. Nat Rev Cancer 9, 338-50 (2009).**
10. **Pommier, Y. Topoisomerase I inhibitors: camptothecins and beyond. Nat Rev Cancer 6, 789-802 (2006).**
11. **Vance, J. R. & Wilson, T. E. Yeast Tdp1 and Rad1-Rad10 function as redundant pathways for repairing Top1 replicative damage. Proc.Natl.Acad.Sci.U.S.A 99, 13669-13674 (2002).**
12. **Liu, C., Pouliot, J. J. & Nash, H. A. Repair of topoisomerase I covalent complexes in the absence of the tyrosyl-DNA phosphodiesterase Tdp1. Proc Natl Acad Sci U S A 99, 14970-5 (2002).**
13. **Pype, S. et al. TTRAP, a novel protein that associates with CD40, tumor necrosis factor (TNF) receptor-75 and TNF receptor-associated factors (TRAFs), and that inhibits nuclear factor-kappa B activation. J Biol Chem 275, 18586-93 (2000).**
14. **Rodrigues-Lima, F., Josephs, M., Katan, M. & Cassinat, B. Sequence analysis identifies TTRAP, a protein that associates with CD40 and TNF receptor-associated factors, as a member of a superfamily of divalent cation-dependent phosphodiesterases. Biochem Biophys Res Commun 285, 1274-9 (2001).**
15. **Nitiss, J. L. et al. Amsacrine and etoposide hypersensitivity of yeast cells overexpressing DNA topoisomerase II. Cancer Res 52, 4467-72 (1992).**
16. **Xu, G. L. et al. TTRAP is a novel PML nuclear bodies-associated protein. Biochem Biophys Res Commun 375, 395-8 (2008).**
17. **Mielke, C., Christensen, M. O., Barthelmes, H. U. & Boege, F. Enhanced processing of UVA-irradiated DNA by human topoisomerase II in living cells. J Biol Chem 279, 20559-62 (2004).**
18. **Mielke, C., Kalfalah, F. M., Christensen, M. O. & Boege, F. Rapid and prolonged stalling of human DNA topoisomerase I in UVA-irradiated genomic areas. DNA Repair (Amst) 6, 1757-63 (2007).**
19. **Kingma, P. S. & Osheroff, N. The response of eukaryotic topoisomerases to DNA damage. Biochim Biophys Acta 1400, 223-32 (1998).**
20. **Connelly, J. C. & Leach, D. R. Repair of DNA covalently linked to protein. Mol.Cell 13, 307-316 (2004).**

21. **Hartsuiker, E., Neale, M. J. & Carr, A. M. Distinct requirements for the Rad32(Mre11) nuclease and Ctp1(CtIP) in the removal of covalently bound topoisomerase I and II from DNA. Mol Cell 33, 117-23 (2009).**

22. **Pei, H. et al. EAPII interacts with ETS1 and modulates its transcriptional function. Oncogene 22, 2699-709 (2003).**

23. **Esguerra, C. V. et al. Ttrap is an essential modulator of Smad3-dependent Nodal signaling during zebrafish gastrulation and left-right axis determination. Development 134, 4381-93 (2007).**

24. **Zucchelli, S. et al. Aggresome-forming TTRAP mediates pro-apoptotic properties of Parkinson's disease-associated DJ-1 missense mutations. Cell Death Differ 16, 428-38 (2009).**

25. **Vance, J. R. & Wilson, T. E. Repair of DNA strand breaks by the overlapping functions of lesion-specific and non-lesion-specific DNA 3' phosphatases. Mol.Cell Biol. 21, 7191-7198 (2001).**

26. **Nitiss, K. C., Malik, M., He, X., White, S. W. & Nitiss, J. L. Tyrosyl-DNA phosphodiesterase (Tdp1) participates in the repair of Top2-mediated DNA damage. Proc Natl Acad Sci U S A 103, 8953-8 (2006).**

27. **Whitehouse, C. J. et al. XRCC1 stimulates human polynucleotide kinase activity at damaged DNA termini and accelerates DNA single-strand break repair. Cell 104, 107-17 (2001).**

28. **Parsons, J. L., Dianova, II & Dianov, G. L. APE1 is the major 3'-phosphoglycolate activity in human cell extracts. Nucleic Acids Res 32, 3531-6 (2004).**

29. **Reynolds, J. J. et al. Defective DNA ligation during short-patch single-strand break repair in ataxia oculomotor apraxia-1. Mol Cell Biol (2008).**

30. **Katyal, S. et al. TDP1 facilitates chromosomal single-strand break repair in neurons and is neuroprotective in vivo. Embo J 26, 4720-31 (2007).**

Figure 1

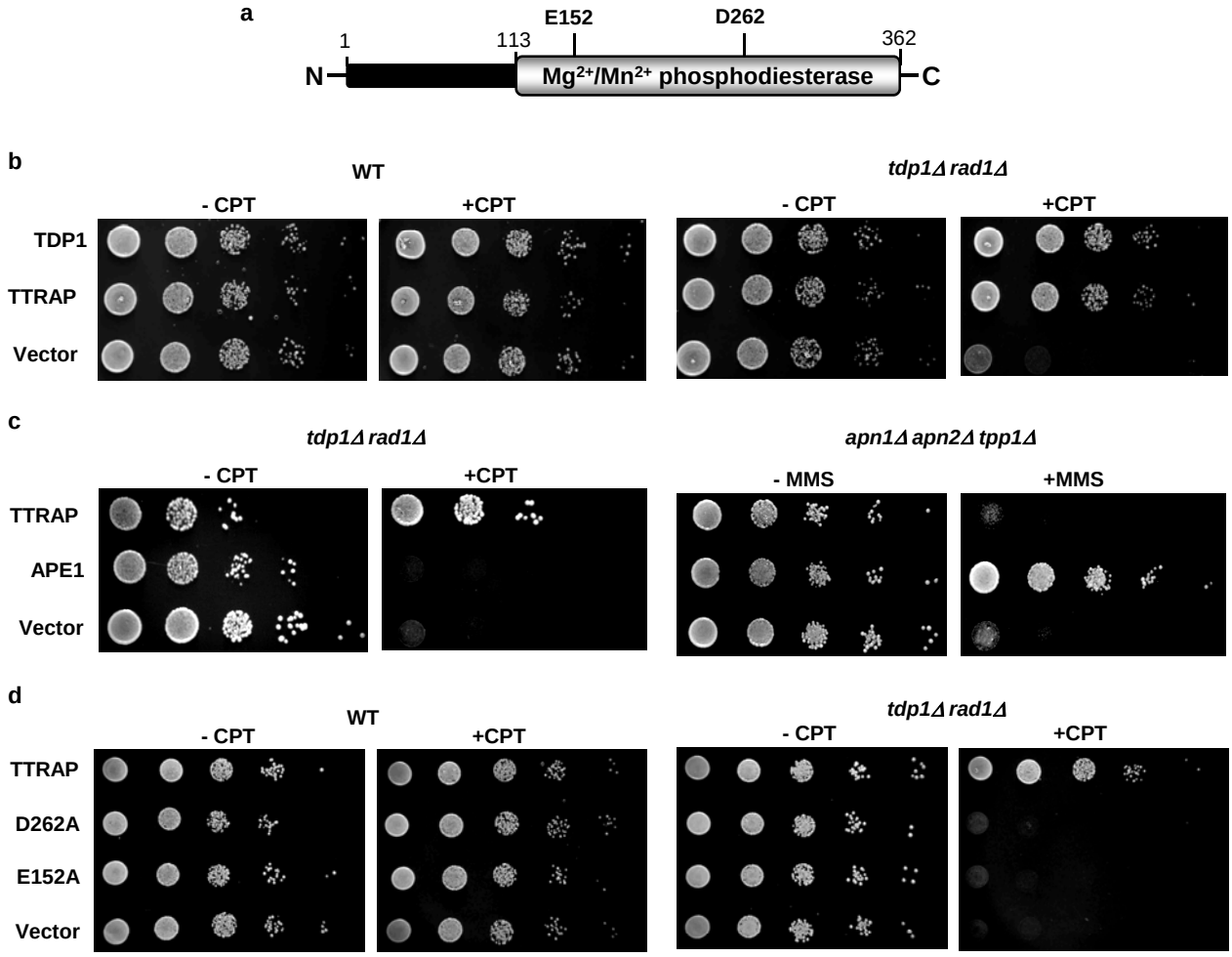
a
E152
D262
1
113
362
N
Mg2+/Mn2+ phosphodiesterase
C
b
WT
tdp1Δ rad1Δ
- CPT
+CPT
- CPT
+CPT
TDP1
TTRAP
Vector
c
tdp1Δ rad1Δ
apn1Δ apn2Δ tpp1Δ
- CPT
+CPT
- MMS
+MMS
TTRAP
APE1
Vector
d
WT
tdp1Δ rad1Δ
- CPT
+CPT
- CPT
+CPT
TTRAP
D262A
E152A
Vector

Figure 2

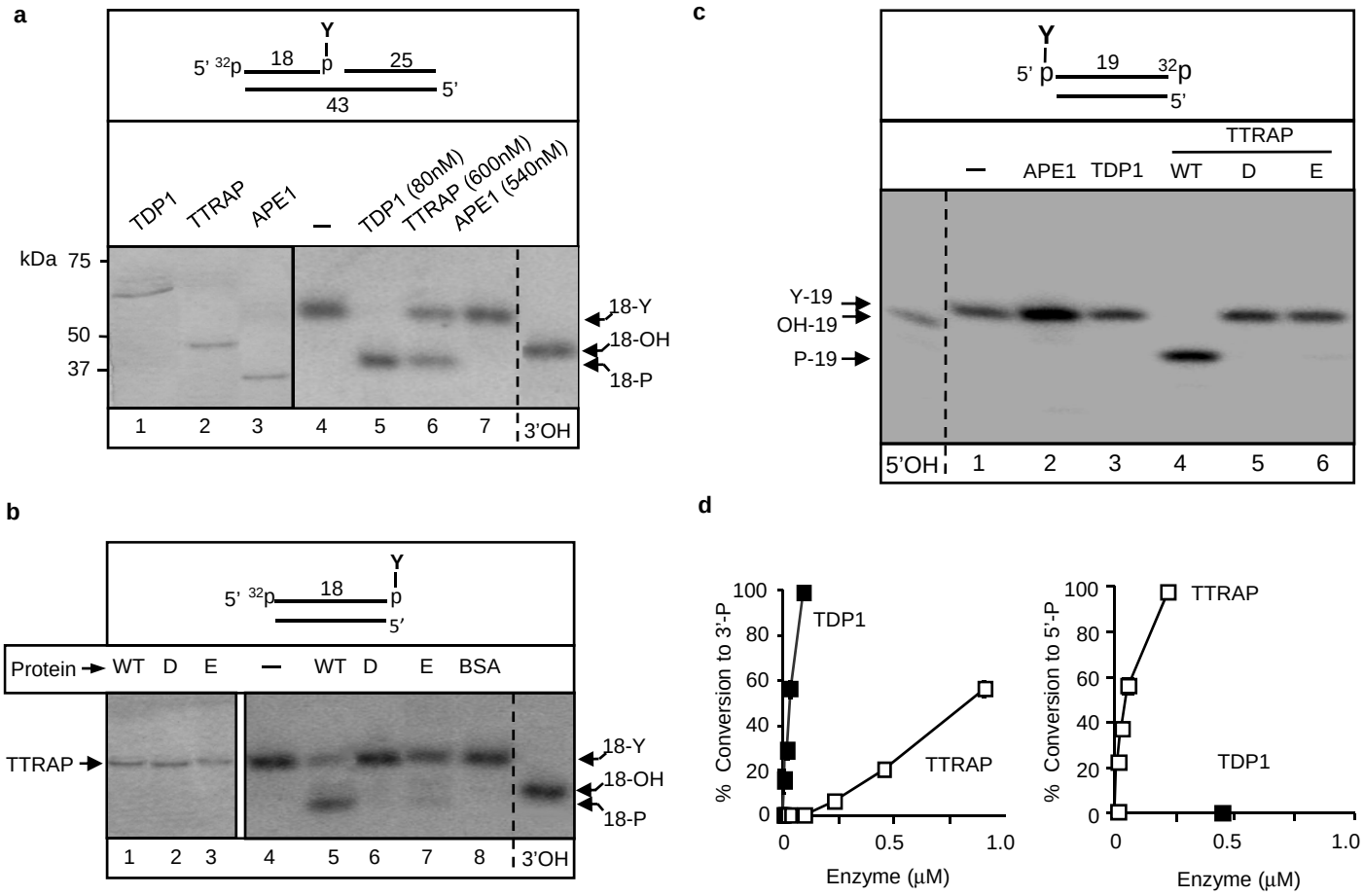
a
Y
5' 32p 18 p 25
43 5'
TDP1
TTRAP
APE1
–
TDP1 (80nM)
TTRAP (600nM)
APE1 (540nM)
kDa 75
50
37
18-Y
18-OH
18-P
1 2 3 4 5 6 7 3'OH
b
Y
5' 32p 18 p
5'
Protein → WT D E – WT D E BSA
TTRAP →
18-Y
18-OH
18-P
1 2 3 4 5 6 7 8 3'OH
c
Y
5' p 19 32p
5'
TTRAP
– APE1 TDP1 WT D E
Y-19
OH-19
P-19 →
5'OH 1 2 3 4 5 6
d
% Conversion to 3'-P
100
80
60
40
20
0
TDP1
TTRAP
0 0.5 1.0
Enzyme (μM)
% Conversion to 5'-P
100
80
60
40
20
0
TTRAP
TDP1
0 0.5 1.0
Enzyme (μM)

Figure 3

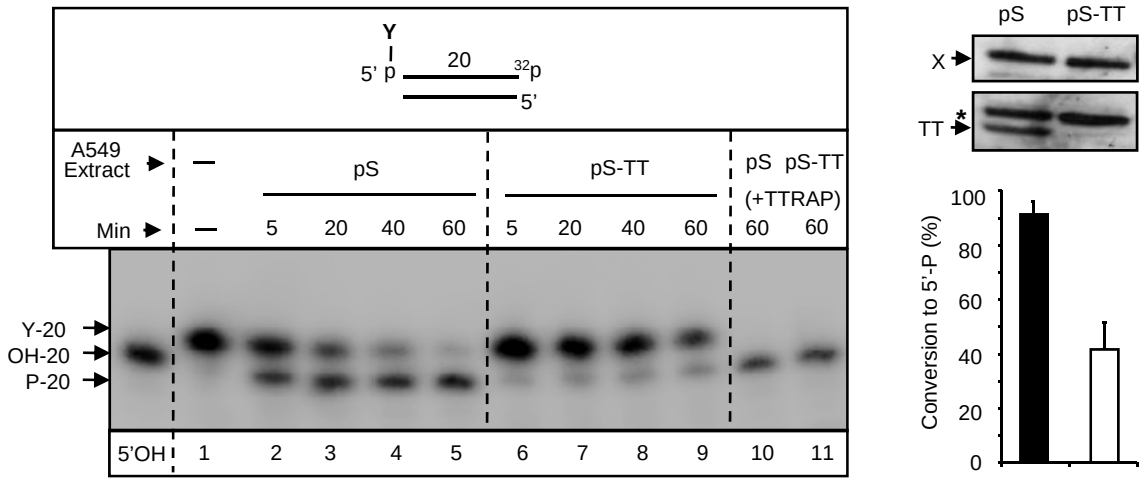
Y
5' p
20
32p
5'
A549 Extract
Min
pS
pS-TT
5
20
40
60
pS
pS-TT
(+TTRAP)
60
60
Y-20
OH-20
P-20
5'OH
1
2
3
4
5
6
7
8
9
10
11
pS
pS-TT
X
TT
*
Conversion to 5'-P (%)
100
80
60
40
20
0

Figure 4

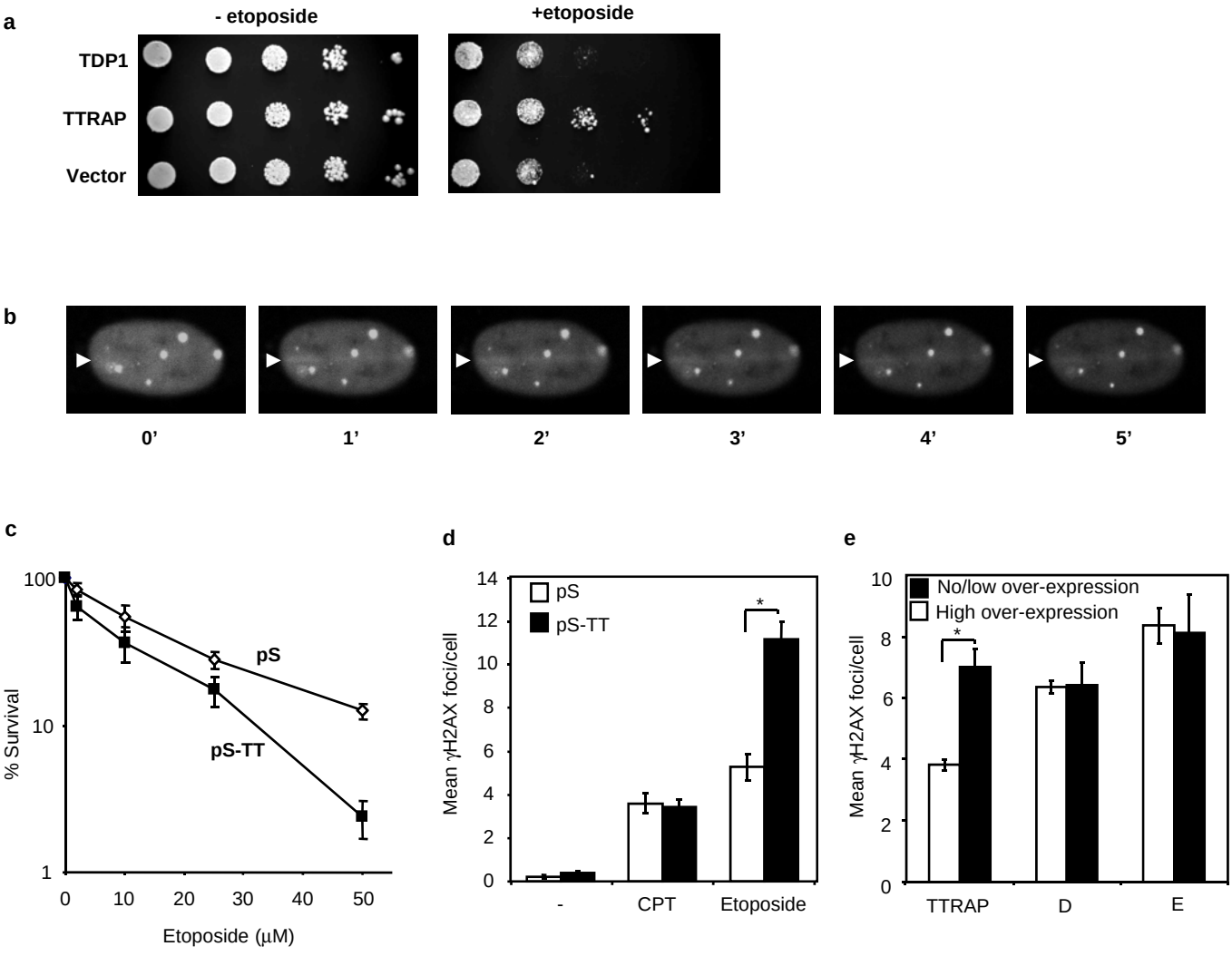
a
- etoposide
+etoposide
TDP1
TTRAP
Vector
b
0’
1’
2’
3’
4’
5’
c
% Survival
100
10
1
pS
pS-TT
0
10
20
30
40
50
Etoposide (μM)
d
Mean γH2AX foci/cell
pS
pS-TT
*
14
12
10
8
6
4
2
0
-
CPT
Etoposide
e
Mean γH2AX foci/cell
No/low over-expression
High over-expression
*
10
8
6
4
2
0
TTRAP
D
E